Hindawi
Complexity
Volume 2021, Article ID 5510428, 10 pages
https://doi.org/10.1155/2021/5510428

Research Article

Assessing the Effectiveness of Mass Testing and Quarantine in the Spread of COVID-19 in Beijing and Xinjiang, 2020

Feng Li,[1,2] Zhen Jin,[3] and Juan Zhang[3]

[1]*Data Science and Technology, North University of China, Taiyuan 030051, China*
[2]*College of Arts and Sciences, Shanxi Agricultural University, Taiyuan 030801, China*
[3]*Complex System Research Center, Shanxi University, Taiyuan, Shanxi 030006, China*

Correspondence should be addressed to Zhen Jin; jinzhn@263.net

Received 24 January 2021; Revised 4 March 2021; Accepted 15 March 2021; Published 31 March 2021

Academic Editor: xiaoke xu

Coronavirus disease (COVID-19) cases and COVID-19-related deaths have been increasing worldwide since the outbreak in 2019. Before the mass vaccination campaign for COVID-19, the main methods for COVID-19 control in China were mass testing and quarantine. Based on the transmission mechanism of COVID-19, we constructed a dynamic model for COVID-19 transmission in two typical regions: Beijing and Xinjiang. We calculated the basic reproduction number R_0, proved the global stability of COVID-19 transmission via the Lyapunov function technique, and introduced the final size. We assessed the effectiveness of mass testing and quarantine. Sensitivity analysis indicated that the more the people were tested per day, the larger is the quarantine proportionality coefficient, the earlier the source location was determined, and the better is the controlling effect. In addition, it was more effective to increase the coefficient of quarantine if the population density in the region was low. To eliminate the pandemic, the government has to expand testing and quarantine, requiring a large amount of continuous manpower, material, and financial resources. Therefore, new control measures should be developed.

1. Introduction

The sudden and unexpected outbreak of the coronavirus disease (COVID-19) pandemic is the most serious global public health emergency and has spread to more than 200 countries. COVID-19 is a contagious respiratory illness caused by the severe acute respiratory syndrome coronavirus 2 (SARS-CoV-2), which is a zoonotic virus. The symptoms of COVID-19 include fever or chills, cough, dyspnea, difficulty in breathing, fatigue, headache, nasal congestion or runny nose, muscle or body aches, sore throat, loss of smell or taste, nausea or vomiting, and diarrhea. Notably, some people become infected but do not develop any symptoms or feel unwell. Infectious droplets are released when someone with COVID-19 sneezes, coughs, or talks, which can settle in the mouth or nose of people who are nearby or possibly be inhaled into the lungs. COVID-19 is thought to spread mainly through close person-to-person contact (within approximately 6 feet). People who are infected but do not show symptoms may also spread the virus to others [1, 2].

In December 2019, COVID-19 was first reported in Wuhan, the capital of Hubei Province in central China. Early in the outbreak, many patients were reported to have a link with a large seafood and live animal market [3, 4]. On January 23, 2020, the Wuhan shutdown was implemented to limit the movement of people in and out of the city. Meanwhile, suspected and confirmed cases had been isolated, public transport had been suspended, schools and entertainment venues had been closed, public gatherings had been banned, and health checks and information had been widely disseminated [5, 6]. Through the lockdown, the spread of the virus was controlled. Residents returned to their normal lives 7 months after the city's strict lockdown was lifted.

In June and July 2020, COVID-19 affected Beijing and Xinjiang Uygur Autonomous Region (for Xinjiang), respectively, giving rise to the second wave of infections; however, this wave was localized within the regions and did not cause widespread transmission. The two regions curbed the rapid spread of COVID-19 cases by adopting strict

prevention and control measures. The details are as follows: on June 11, 2020, a new locally transmitted case was reported in Beijing. The Xinfadi wholesale market, which is the largest food wholesale market in Beijing, was identified as a possible source of infection within 22 hours. Most cases were linked to the market. The market was shut down, high-risk individuals were identified, and nearby communities were subjected to lockdown. The government ensured an increase in COVID-19 testing, including testing of suspected persons, and followed up on their status. With the implementation of targeted measures, Beijing controlled the surge in cases in less than a month. The number of daily infections returned to zero by July 7. The market was reopened to the public on August 16. On July 15, 2020, a 24-year-old woman from Urumqi (the capital of Xinjiang) tested positive for SARS-CoV-2, making her the first locally transmitted COVID-19 case in Xinjiang since February. Based on epidemiological investigations and laboratory testing, this round of outbreak was associated with a gathering, and most confirmed cases were reported in Urumqi. No newly confirmed or asymptomatic COVID-19 cases have been reported in Xinjiang since August 16. Before the mass vaccination campaign of COVID-19, there was successful management of the outbreak in Wuhan, which offered a valuable experience to those in Beijing and Xinjiang. Expanding the testing of the population and asking people from medium- and high-risk areas or who had close contact with confirmed or asymptomatic cases to quarantine themselves gated widespread community spread or spread across regions. These measures have effectively reduced the spread of the virus and prevented mass infections, thereby helping consolidate the efforts of COVID-19 control and prevention. These two outbreaks were quickly curbed. However, the time of pandemic control in Xinjiang was longer than that in Beijing.

With the massive global pandemic, it is natural that the outbreak emerges accidentally in other areas worldwide. There are geographical, economic, cultural, health care, and population density differences between people living in Beijing and Xinjiang. For instance, the population density in Beijing is about 1313 people per square kilometer, whereas it is 14.98 people per square kilometer in Xinjiang. Based on the initial spread of the infection, in Beijing, the source of the infection, that is, the market, was identified within 22 hours after the first case was confirmed. In Xinjiang, the epidemiological analysis showed that the virus source of this outbreak was from the same source of infection identified 13 days later. The other regions can learn from these two regions' experiences in containing the spread of the virus. Quantifying the effectiveness of these control measures is of crucial importance for cities preparing for rapid responses in the event of another outbreak; if asymptomatic cases are identified quickly, the source of the infection can be controlled and the infection rate can be reduced. Therefore, massive screening of asymptomatic cases and quarantine of susceptible people in communities are necessary.

The dynamic model is a useful method for identifying the key factors affecting disease outbreaks and evaluating the intervention strategies. Based on the transmission mechanism, the model can dynamically predict future trends according to current information. The quantities used often include the basic or effective reproduction number and the final epidemic size [7–11]. A mathematical model is used to estimate the degree of the COVID-19 epidemic in cities worldwide [12–16]. The SEIR model is the most widely adopted model to study the COVID-19 outbreak in China and other countries [17–20]. Based on the SEIR model, some researchers have increased the number of states that have to follow the quarantine process [6, 21]. We analyzed the transmission of COVID-19 in two typical regions: Beijing and Xinjiang. Between the two regions, the outbreak occurred simultaneously and similar control measures were adopted, though there were significant differences, for instance, in the duration of confirming the source, the ability of mass testing, and proportional coefficient of quarantine.

In this study, we considered a dynamic model with intervention measures. The model is introduced in Section 2. In Section 3, the basic reproduction number, R_0, a threshold quantity for the stability of equilibria, was calculated. Using the Lyapunov function, we proved that the disease-free equilibrium was globally asymptotically stable if $R_0 \leq 1$, whereas an endemic equilibrium was globally asymptotically stable if $R_0 > 1$. The final size was derived. In Section 4, we estimate the parameter values using Markov Chain Monte Carlo (MCMC) simulations. In Section 5, we explore the influence of mass testing and quarantine in Beijing and Xinjiang. The final size was evaluated for COVID-19 in Beijing and Xinjiang.

2. Model Formulation

The SIHRS$_q$ model was used to estimate the COVID-19 epidemic in Beijing and Xinjiang. We divided the total population (N) into five groups: susceptible (S), unfound infected (I), hospitalized (H), removed (R, removed group includes recovered and death populations), and quarantine (S_q). Susceptible people were infected by asymptomatic infected people. Through a latent period, some infected people developed symptoms, went to the hospital, and were diagnosed, while others remained asymptomatic. Some asymptomatic people who were identified by nucleic acid testing were taken to the hospital. Therefore, hospitalized patients included symptomatic and asymptomatic individuals. Patients hospitalized were isolated and treated; thus, we considered that the susceptible people could not be infected by the hospitalized patients. Other asymptomatic people not diagnosed in the crowd recovered without treatment. Recovered patients included the treated and untreated patients. To minimize risks, susceptible people from medium- and high-risk areas or who had close contact with confirmed or asymptomatic cases were tested. If their results were negative on nucleic acid testing, they were prohibited from leaving the outbreak regions and quarantined. Therefore, the susceptible individuals were quarantined in proportion to the number of new cases hospitalized. Those quarantined remained till the outbreak was over in their regions. Hence, people quarantined did move toward susceptible people.

Based on the previous assumptions, the dynamic model was described by the following ordinary differential equations:

$$\begin{cases} \dfrac{\mathrm{d}S(t)}{\mathrm{d}t} = -\beta\dfrac{S}{N}I - \kappa_q\dfrac{S}{N}I + \mu N - \mu S, \\ \dfrac{\mathrm{d}I(t)}{\mathrm{d}t} = \beta\dfrac{S}{N}I - \alpha_1 I - \alpha_2 I - \mu I, \\ \dfrac{\mathrm{d}H(t)}{\mathrm{d}t} = \alpha_1 I - \delta H - \mu H, \\ \dfrac{\mathrm{d}R(t)}{\mathrm{d}t} = \alpha_2 I + \delta H - \mu R, \\ \dfrac{\mathrm{d}S_q(t)}{\mathrm{d}t} = \kappa_q\dfrac{S}{N}I - \mu S_q, \end{cases} \tag{1}$$

where $\alpha_2 = \gamma(1-\rho)(1-\lambda)$, $\alpha_1 = \rho(1-\lambda)+\lambda$, and $\kappa_q = \kappa(1-\beta)\alpha_1$, where β is the infection coefficient. λ denotes the discovery rate of infectious people. γ and δ are the recovery rates. $1/\mu$ is the rate of natural births and deaths, where ρ is the daily proportion of nucleic acid testing. With contact tracing, the uninfected individuals, who got in contact with new hospitalized cases, move to the quarantined compartment at a rate of κ_q. All parameters were nonnegative. A flow diagram of system (1) is shown in Figure 1. Additionally, the total population was included $N(t) = S(t) + I(t) + H(t) + R(t) + S_q(t)$. Adding all five equations in system (1), we obtain $(\mathrm{d}N/\mathrm{d}t) = 0$, for all $t \geq 0$, which implies $N(t) = N(0) > 0$ for all $t \geq 0$. Let the feasible region for system (1) be

$$\Omega = \left\{\left(S, I, H, R, S_q\right) \in R_+^5 : 0 < S + I + H + R + S_q \leq N\right\}. \tag{2}$$

And the initial condition is

$$\begin{aligned} S(0) = S^0 \geq 0, \quad & I(0) = I^0 \geq 0, \\ H(0) = H^0 \geq 0, \quad & S_q(0) = S_q^0 \geq 0, \\ & R(0) = R^0 \geq 0, \\ N(0) = N^0 = S^0 + I^0 + H^0 + R^0 + S_q^0. & \end{aligned} \tag{3}$$

Theorem 1. *The region Ω is positively invariant with respect to system (1).*

Proof. To show the positivity of each individual, we first show that $I(t) > 0$. We multiply both sides of the second equation of system (1) by $\Theta(t) = e^{-\int_0^t (\beta(S(\tau)/N))\mathrm{d}\tau + (\alpha_1+\alpha_2+\mu)t}$ and obtain

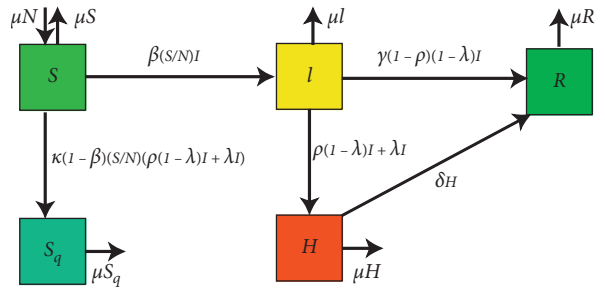

Figure 1: General transfer diagram of the model.

$$\Theta(t)I'(t) = \Theta(t)\left(\beta\frac{S(t)}{N} - (\alpha_1 + \alpha_2 + \mu)\right)I(t). \tag{4}$$

We obtain

$$I(t) = I^0 e^{\int_0^t (\beta(S(\tau)/N))\mathrm{d}\tau - (\alpha_1+\alpha_2+\mu)t}. \tag{5}$$

Since $I^0 \geq 0$, we obtain $I(t) \geq 0$ for all time $t > 0$. Now to show that $H(t) > 0$, we multiply both sides of the third equation of system (1) with $e^{(\delta+\mu)t}$ and obtain

$$e^{(\delta+\mu)t}H\prime(t) = e^{(\delta+\mu)t}(\alpha_1 I(t) - (\delta+\mu)H(t)). \tag{6}$$

We may write

$$\left(e^{(\delta+\mu)t}H(t)\right)' = e^{(\delta+\mu)t}\alpha_1 I(t), \tag{7}$$

on integrating from 0 to t and get

$$H(t) = e^{-(\delta+\mu)t}H^0 + \int_0^t e^{(\delta+\mu)(\tau-t)}\alpha_1 I(\tau)\mathrm{d}\tau. \tag{8}$$

Since $H^0 \geq 0$ and $I(t) \geq 0$ for all times $t > 0$, we have $H(t) > 0$. We multiply both sides of the fourth equation of system (1) by $e^{\mu t}$. By integrating from 0 to t, we obtain

$$R(t) = e^{-\mu t}\left(R^0 + \int_0^t (\alpha_2 I(\tau) + \delta H(\tau))\mathrm{d}\tau\right). \tag{9}$$

Because $R^0 \geq 0$, $I(t) \geq 0$, and $H(t) \geq 0$ for all times $t > 0$, we have $R(t) > 0$. From the fifth equation of system (1) and $S = N - I - H - R - S_q$, we obtain

$$S_q'(t) = \kappa_q\frac{N - I(t) - H(t) - R(t)}{N}I(t) - \left(\kappa_q\frac{I(t)}{N} + \mu\right)S_q(t). \tag{10}$$

We multiply both sides of the above equation with $\Phi(t) = e^{\int_0^t (\kappa_q(I(\tau)/N))\mathrm{d}\tau + \mu t} > 0$ and get

$$\left(\Phi(t)S_q(t)\right)' = \kappa_q\Phi(t)\frac{N - I(t) - H(t) - R(t)}{N}I(t). \tag{11}$$

On integrating from 0 to t, we obtain that

$$S_q(t) = \Phi^{-1}(t)\left(S_q^0 + \int_0^t \left(\kappa_q \Phi(\tau)\frac{N - I(\tau) - H(\tau) - R(\tau)}{N} I(\tau)\right)\mathrm{d}\tau\right). \tag{12}$$

Since $S_q^0 \geq 0, N - I(t) - H(t) - R(t) \geq 0$, and $I(t) \geq 0$ for all times $t > 0$, we have $S_q(t) > 0$. Similarly, to show that $S(t) > 0$, we multiply both sides of the first equation of system (1) by $\Psi(t) = e^{\int_0^t (\beta(I(\tau)/N) + \kappa_q(I(\tau)/N) + \mu)\mathrm{d}\tau} > 0$ and obtain

$$\Psi(t)S'(t) = \Psi(t)\mu N - \Psi(t)\left(\beta\frac{I(t)}{N} + \kappa_q\frac{I(t)}{N} + \mu\right)S(t), \tag{13}$$

which can be rewritten as

$$(\Psi(t)S(t))' = \mu N \Psi(t). \tag{14}$$

On integrating from 0 to t, we obtain that

$$S(t) = \Psi^{-1}(t)\left(S^0 + \int_0^t \mu N \Psi(\tau)\mathrm{d}\tau\right), \tag{15}$$

and thus $S(t) > 0$ for all times $t > 0$.

$N(t) = N$. Therefore, the region Ω is positively invariant. The solution enters Ω in an infinite time or $N(t)$ asymptotically approaches N. The region Ω attracts all solutions in R_+^5 [22]. □

3. Dynamical Analysis

For the convenience of calculation, adding the equations in system (1), it follows that $N(t)$ is a first integral, and introducing the densities $s = (S/N)$, $i = (I/N)$, $h = (H/N)$, $s_q = (S_q/N)$, $r = (R/N)$, and $s + i + h + s_q + r = 1$, system (1) becomes

$$\begin{cases} \dfrac{\mathrm{d}s(t)}{\mathrm{d}t} = \mu - \beta si - \kappa_q si - \mu s, \\ \dfrac{\mathrm{d}i(t)}{\mathrm{d}t} = \beta si - (\alpha_1 + \alpha_2)i - \mu i, \\ \dfrac{\mathrm{d}h(t)}{\mathrm{d}t} = \alpha_1 i - \delta h - \mu h, \\ \dfrac{\mathrm{d}r(t)}{\mathrm{d}t} = \alpha_2 i + \delta h - \mu r, \\ \dfrac{\mathrm{d}s_q(t)}{\mathrm{d}t} = \kappa_q si - \mu s_q. \end{cases} \tag{16}$$

3.1. Global Stability of the Disease-Free Equilibrium (DFE). By solving the equations of system (16) at a steady state, we obtain a disease-free equilibrium (DFE) $P^0 = (s^0, 0, 0, 0, 0)$, where $s^0 = 1$. We can evaluate the basic reproduction number R_0 for system (16) following the next-generation matrix formulated by van den Driessche and Watmough [23]. For the epidemic model, R_0 shows that an average of each infected individual infects more than one individual. If $R_0 \leq 1$, the disease dies out. On the other hand, we may expect the disease to spread in the community if $R_0 > 1$. The basic reproduction number R_0 for system (16) is

$$R_0 = \frac{\beta}{\alpha_1 + \alpha_2 + \mu}. \tag{17}$$

Theorem 2. *The DFE of system (32) is locally asymptotically stable if $R_0 \leq 1$ and unstable if $R_0 > 1$.*

Proof. By linearizing system (16) around P^0, the local stability of the DFE solution can be examined. Let $x = (i, h, r, s_q, s)$ and $f(x)$ denote the vector field of the system in (16). Jacobian matrix $J = (\partial f/\partial x)$ associated with this P^0:

$$J|_{P^0} = \begin{pmatrix} \beta - \alpha_1 - \alpha_2 - \mu & 0 & 0 & 0 & 0 \\ \alpha_1 & -\delta - \mu & 0 & 0 & 0 \\ \alpha_2 & \delta & -\mu & 0 & 0 \\ \kappa_q & 0 & 0 & -\mu & 0 \\ -\beta - \kappa_q & 0 & 0 & 0 & -\mu \end{pmatrix}. \tag{18}$$

The characteristic equation for the above matrix is

$$(\lambda + \mu)^3 (\lambda + (\alpha_1 + \alpha_2 + \mu)(1 - R_0))(\lambda + \delta + \mu) = 0. \tag{19}$$

We can see that all the eigenvalues have negative real parts if and only if $R_0 < 1$ which shows that the DFE P^0 is locally asymptotically stable. The DFE P^0 is unstable if $R_0 > 1$. □

Theorem 3. *The DFE of system (16) is globally asymptotically stable in Ω whenever $R_0 < 1$.*

Proof. Consider the following Lyapunov function:

$$V(t) = i(t). \tag{20}$$

Then, if $R_0 < 1$,

$$\begin{aligned} V'(t) &= i'(t) \\ &= \beta si - (\alpha_1 + \alpha_2 + \mu)i \\ &\leq (\beta - \alpha_1 - \alpha_2 + \mu)i \\ &= (\alpha_1 + \alpha_2 - \mu)(R_0 - 1), \quad i \leq 0, \end{aligned} \tag{21}$$

where $V' = 0$ if and only if $i = 0$. The largest compact invariant set in $\{(s, i, h, r, s_q) \in \Omega: V\prime = 0\}$ is a singleton P^0. The global stability of P^0 follows from LaSalle's invariance principle [24–26]. This establishes the theorem. □

3.2. Global Stability of the Endemic Equilibrium. By solving the equations of system (16) in the steady state, there is an endemic equilibrium $P^* = (s^*, i^*, h^*, r^*, s_q^*)$ if $R_0 > 1$, where

$$\begin{aligned} s^* &= \frac{1}{R_0} > 0, \\ i^* &= \frac{(R_0 - 1)\mu}{\beta + \kappa_q} > 0, \\ h^* &= \frac{\alpha_1}{\delta + \mu} i^* > 0, \\ r^* &= \frac{\delta\alpha_1 + (\delta + \mu)\alpha_2}{(\delta + \mu)\mu} i^* > 0, \\ s_q^* &= \frac{(R_0 - 1)\kappa_q(\mu + \alpha_1 + \alpha_2)}{\beta(\beta + \kappa_q)} > 0. \end{aligned} \tag{22}$$

Now, we prove that P^* is globally asymptotically stable in the interior of Ω. We establish the following result.

Theorem 4. *The unique endemic equilibrium P^* is locally asymptotically stable if $R_0 > 1$.*

Proof. By linearizing system (16) about P^*, we obtain the Jacobian matrix:

$$J|_{P^*} = \begin{pmatrix} \beta s^* - \alpha_1 - \alpha_2 - \mu & 0 & 0 & 0 & \beta i^* \\ \alpha_1 & -\delta - \mu & 0 & 0 & 0 \\ \alpha_2 & \delta & -\mu & 0 & 0 \\ \kappa_q s^* & 0 & 0 & -\mu & 0 \\ -(\beta + \kappa_q) s^* & 0 & 0 & 0 & -(\beta + \kappa_q) i^* - \mu \end{pmatrix}. \tag{23}$$

The characteristic equation for the above matrix is

$$(\lambda + M_1)(\lambda + M_2)(\lambda + \mu)(\lambda + \eta + \mu)(\lambda + \delta + \mu) = 0, \tag{24}$$

where

$$\begin{aligned} M_1 &= \frac{(\beta + \kappa_q)(\alpha_1 + \alpha_2 + \mu) i^*}{(\beta + \kappa_q) i^* + \mu}, \\ M_2 &= (\beta + \kappa_q) i^* + \mu. \end{aligned} \tag{25}$$

Hence, all the eigenvalues are negative real parts if $R_0 > 1$, which shows that P^* is locally asymptotically stable. □

Theorem 5. *The endemic equilibrium P^* is globally asymptotically stable whenever $R_0 > 1$.*

Proof. We define the following Lyapunov function:

$$V = s^* \int_{s^*}^{s} \frac{\beta\tau - (\alpha_1 + \alpha_2 + \mu)}{\tau} \mathrm{d}\tau + \int_{i^*}^{i} \frac{(\beta + \kappa_q) s^* \tau + \mu s^* - \mu}{\tau} \mathrm{d}\tau, \tag{26}$$

where $\alpha_1 + \alpha_2 + \mu = \beta s^*$. By calculating the time derivative of V along the solution of system (16), we obtain

$$V' = -\frac{\mu\beta(s - s^*)^2}{s} \leq 0, \tag{27}$$

for all $(s, i) \in \Omega$. Therefore, (s^*, i^*) is globally asymptotically stable.

Using the previous conclusion,

$$h(t) = e^{-(\delta+\mu)t} h^0 + \int_0^t e^{(\delta+\mu)(\tau - t)} \alpha_1 i(\tau) \mathrm{d}\tau. \tag{28}$$

We derive

$$\lim_{t \longrightarrow \infty} h(t) = \lim_{t \longrightarrow \infty} \frac{\alpha_1 i(t)}{\delta + \mu} = i^*. \tag{29}$$

Similarly, we obtain

$$\begin{aligned} \lim_{t \longrightarrow \infty} r(t) &= r^*, \\ \lim_{t \longrightarrow \infty} s_q(t) &= s_q^*. \end{aligned} \tag{30}$$

According to LaSalle's invariance principle [27, 28], the endemic equilibrium P^* is unique and globally asymptotically stable in the interior of Ω if $R_0 > 1$. The theorem is proven. □

3.3. Final Size. The final size of the epidemic is the number of individuals ultimately becoming infected, which is the total number of cases during the entire outbreak [29, 30]. In analyzing system (16), we adopt the conventions that, for an arbitrary continuous function $x(t)$ with nonnegative components:

$$x^{\infty} = \lim_{t \longrightarrow \infty} x. \tag{31}$$

Due to the small-time span, we considered natural birth and death to be zero.

Letting $\mu = 0$ in system (16), it becomes

$$\begin{cases} \dfrac{\mathrm{d}s(t)}{\mathrm{d}t} = -\beta s i - \kappa_q s i, \\ \dfrac{\mathrm{d}i(t)}{\mathrm{d}t} = \beta s i - (\alpha_1 + \alpha_2) i, \\ \dfrac{\mathrm{d}h(t)}{\mathrm{d}t} = \alpha_1 i - \delta h, \\ \dfrac{\mathrm{d}r(t)}{\mathrm{d}t} = \alpha_2 i + \delta h, \\ \dfrac{\mathrm{d}s_q(t)}{\mathrm{d}t} = \kappa_q s i. \end{cases} \tag{32}$$

The disease basic reproductive number is

$$R_0 = \frac{\beta}{\alpha_1 + \alpha_2}. \tag{33}$$

We observe that

$$\begin{aligned} \left(s(t) + s_q(t)\right)\prime &< 0, \\ \left(s(t) + s_q(t) + i(t)\right)\prime &< 0, \\ \left(s(t) + s_q(t) + i(t) + h(t)\right)\prime &< 0, \\ r\prime(t) &> 0, \end{aligned} \tag{34}$$

for all $t > 0$, while we know that $s(t), s_q(t), i(t), h(t) > 0$ and $0 \le r(t) < N$; hence, s^∞ and r^∞ exist, and we have $i^\infty = 0$, $h^\infty = 0$, and $s_q^\infty = 0$. Adding s, s_q, and i equations to system (32), we obtain

$$\left(s + s_q + i\right)\prime = -(\alpha_1 + \alpha_2)i. \tag{35}$$

Integration of the equation with respect to t from 0 to ∞ gives

$$\int_0^\infty i\mathrm{d}t = \frac{1}{\alpha_1 + \alpha_2}\left(s^0 - s^\infty + s_q^0 + i^0\right). \tag{36}$$

Adding $s$and s_q equations to system (32),

$$\left(s + s_q\right)\prime = -\beta s i. \tag{37}$$

From $(\mathrm{d}i/d(s + s_q))$, we obtain that

$$\begin{aligned} \mathrm{d}i &= -d\left(s + s_q\right) + \frac{1}{R_0}\left(\frac{\mathrm{d}s}{s} + \frac{\mathrm{d}s_q}{s}\right) \\ &= -d\left(s + s_q\right) + \frac{1}{R_0}\frac{\mathrm{d}s}{s} + \frac{\kappa_q}{R_0}i. \end{aligned} \tag{38}$$

An epidemic ends when no infection is found; that is, $i^\infty = 0$, $h^\infty = 0$. The integration of the above equation yields

$$\ln\left(\frac{s^\infty}{s^0}\right) = -R_0\left(1 + \frac{\kappa_q}{\beta}\right)\left(s^0 - s^\infty + s_q^0 + i^0\right). \tag{39}$$

We now derive the equation for the final epidemic size, defined by $Y = s^0 - s^\infty$. This yields an implicit relation:

$$Y = s^0 e^{-R_0\left(1+\left(\kappa_q/\beta\right)\right)\left(Y+s_q^0+i^0\right)}. \tag{40}$$

4. Estimation of Epidemiological Parameters

We obtained data on COVID-19 cases in Beijing and Xinjiang from the National Health Commission of The People's Republic of China. The data included the cumulative and new infections of confirmed, suspected, death, cured, and asymptomatic cases; the cumulative number of close contacts; and hospitalization time [31].

In China, the per-day rate of natural birth and death is $\mu = 0.01094/365$. Suppose that the recovery rate of asymptomatic cases is $\gamma = 1/14$. Beijing is a metropolitan area with a population of 21.536 million ($N = 2.1536 \times 10^7$). From June 11 to July, 9,335 confirmed local cases and 49 asymptomatic cases had been reported, and no deaths were reported of the cases in Beijing. According to the data in Beijing, the mean time from infection to being tested positive for the virus was 10.8 days $\lambda = (1/10.8)$, and the treatment time was 10 days $\delta = (1/10)$. The testing capacity was approximately 0.3 million people per day $\rho = 3 \times 10^5/N$. The initial values on June 11 in Beijing were $S(0) = 2.1536 \times 10^7$ $R(0) = 0$ and $H(0) = 1$.

The population in Xinjiang is 24.87 million ($N = 2.487 \times 10^7$). Since the outbreak of the virus on July 15, 828 confirmed COVID-19 cases and 391 asymptomatic cases have been reported in Xinjiang, mainly in Urumqi. No newly confirmed COVID-19 case had been reported in Xinjiang since August 16. The treatment time was 11 days $\delta = 1/11$. From July 15 to 19, about 0.24 million people who had close contact with infected people and asymptomatic carriers had got the nucleic acid test, where the testing capacity was 0.06 million people per day ($\rho_1 = 6 \times 10^4/N$). The mean time from infection to being tested positive for the virus was 14 days ($\lambda_1 = 1/14$). On July 18, a citywide, free nucleic acid test was launched in Xinjiang. The testing capacity was up to 0.5 million people per day ($\rho_2 = 5 \times 10^5/N$) since July 20, the meantime from getting infected to being tested positive for the virus was shortened ($\lambda_2 = 1/7$). The initial values on June 11 in Xinjiang were $S(0) = 2.487 \times 10^7$, $R(0) = 0$, and $H(0) = 1$.

Based on the mathematical model, the cumulative numbers of confirmed cases and identified asymptomatic cases were determined in Beijing and Xinjiang. We used the MCMC method to fit the model and adopted an adaptive Metropolis–Hastings algorithm to carry out the MCMC procedure. The algorithm was run for 30,000 iterations with a burn-in of the first 10,000 iterations, and the Geweke convergence diagnostic method was employed to assess the convergence of chains [32, 33]. We could acquire the parameter values for β and κ, and the initial values for S_q^0 and I^0 in the two regions. The mean values and 95% confidence intervals (95% CI) are presented in Table 1.

The infection coefficient in Beijing ($\beta = 0.0640$) is lower than that in Xinjiang ($\beta = 0.1522$). S_q^0 in Beijing is greater than that in Xinjiang because the population density in Beijing (approximately 1313 people per square kilometer) is higher than that in Xinjiang (approximately 14.98 people square kilometer). I^0 in Beijing is lower than that in Xinjiang because the source of infection in Beijing was identified quicker than that in Xinjiang. The time evolution of the infected cases and comparison with the cumulative number of confirmed cases and identified asymptomatic cases are shown in Figure 2. Evidently, the theoretical prediction is nearly in agreement with the actual data, which also validates the accuracy of the model. The final sizes of the pandemic in Beijing and Xinjiang were $S(\infty) = 2.1535137 \times 10^7$, $R(\infty) = 862$ and $S(\infty) = 2.4866980 \times 10^7$, $R(\infty) = 3019$, respectively. The final scale in Beijing is smaller.

5. Spread of COVID-19 and the Effectiveness of Interventions in Beijing and Xinjiang

The basic reproduction numbers in Beijing and Xinjiang were 0.3783 and 1.0882, respectively. The basic reproductive

Table 1: Parameter estimation for COVID-19 in Beijing and Xinjiang.

Parameter	Beijing		Xinjiang		Source
	Mean	95% CI	Mean	95% CI	
β	0.0640	[0.0640, 0.0641]	0.1522	[0.1520, 0.1524]	MCMC
κ	99.2342	[93.4580, 105.8892]	83.3883	[83.3727, 83.4038]	MCMC
S_q^0	80.0866	[80.0864, 80.0868]	1.8793	[1.8790, 1.8796]	MCMC
I^0	344.4526	[344.1625, 344.7428]	449.7552	[447.4628, 451.0475]	MCMC

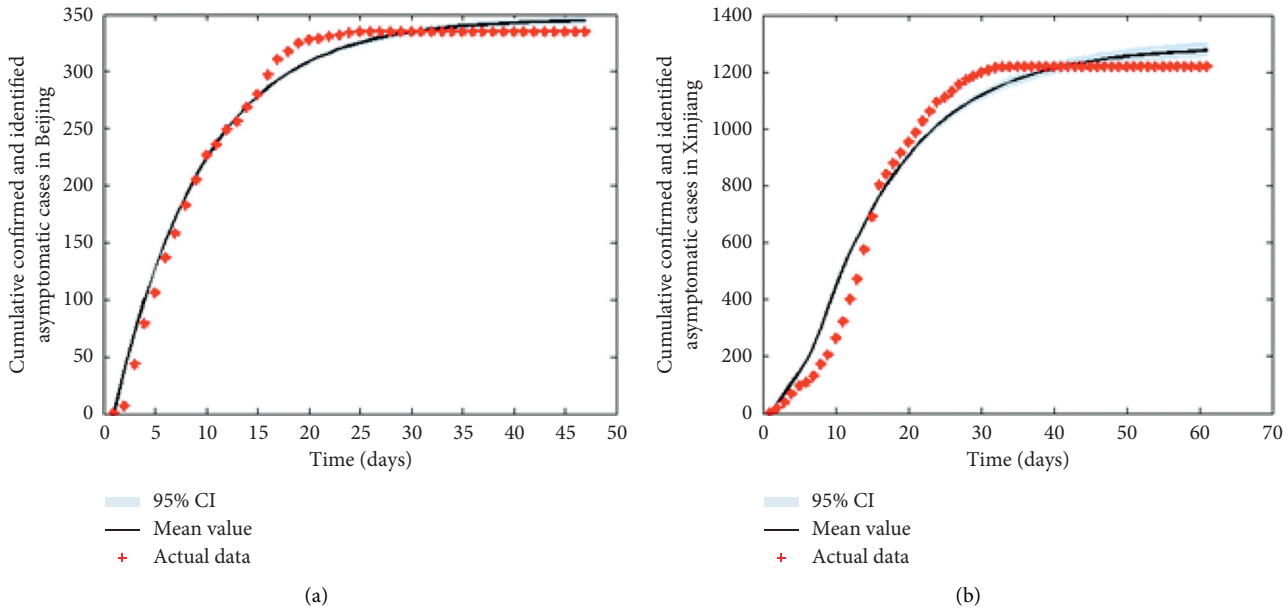

Figure 2: Fitting results of the estimated cumulative number of confirmed and identified asymptomatic COVID-19 cases with its actual reported numbers in Beijing and Xinjiang.

number in Beijing was less than one, and it was verified that the disease dies out. The basic reproductive number in Xinjiang was greater than one; however, with the increasing expansion of the nucleic acid testing, the outbreak was curbed. To draft policies for control measures, we analyzed the cumulative number of confirmed and identified asymptomatic COVID-19 cases for different values of κ (Figure 3). The analysis showed that, to control the spread of COVID-19 (the smaller the final size, the shorter the duration), a larger coefficient of quarantine is necessary. In addition, as the population density in Xinjiang is less than that in Beijing, it is effective to increase the coefficient of quarantine in Xinjiang. We provided a sensitivity analysis of the basic production number R_0 with the parameters β and ρ in Beijing and Xinjiang (Figure 4). Apparently, improving the testing capacity ρ can decrease the basic reproduction number R_0. When the testing capacity reaches a certain level, it will make the basic reproduction number R_0 less than one (Figure 4). In Xinjiang, the basic reproduction number $R_0 > 1$ was equal to $\rho \geq 415600/N$ if the other parameters are fixed. This implies that the infection could not persist over time in Xinjiang if the number of people tested was greater than 415,600 per day. Without mass vaccination campaigns, mass testing may be an effective prevention measure. Early detection of new cases is a useful control strategy for COVID-19.

6. Conclusion and Discussion

In this study, we constructed a mathematical model for COVID-19 transmission in Beijing and Xinjiang in 2020. There are differences in geographical, economic, cultural, health care, and lifestyles of people living in the two regions. The population in Xinjiang is similar to that in Beijing; however, the population density in Xinjiang is 100 times less than that in Beijing. The outbreak occurred in Beijing and then in Xinjiang. Similar measures (mass testing and quarantine) were adopted in the two regions, though the time to confirm the source, the ability of mass testing, and the proportional coefficient of quarantine were different. To explore effective control and prevention measures for COVID-19, we proposed a deterministic model with mass testing and quarantine to describe the spread of COVID-19 in China. First, the basic reproduction number R_0 of the model was provided. Then, it was found that the model had two nonnegative equilibria: the DFE and endemic equilibrium. Through the analysis of the model, it was found that the global behavior of the system was completely determined

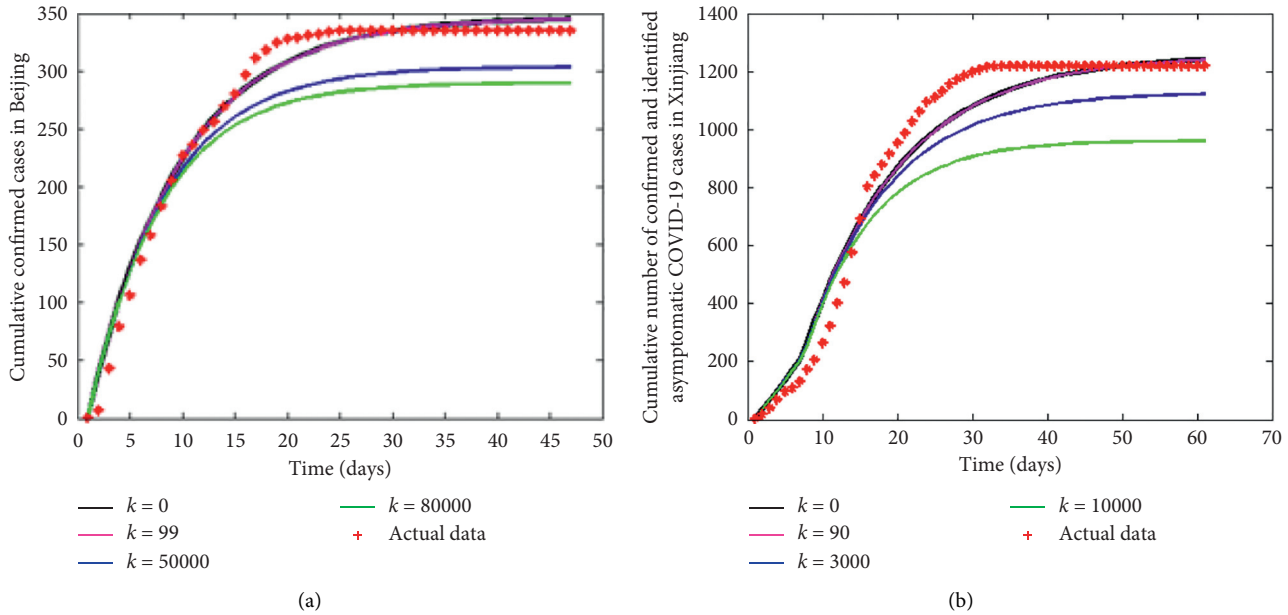

Figure 3: Cumulative number of confirmed and identified asymptomatic COVID-19 cases on κ in (a) Beijing and (b) Xinjiang.

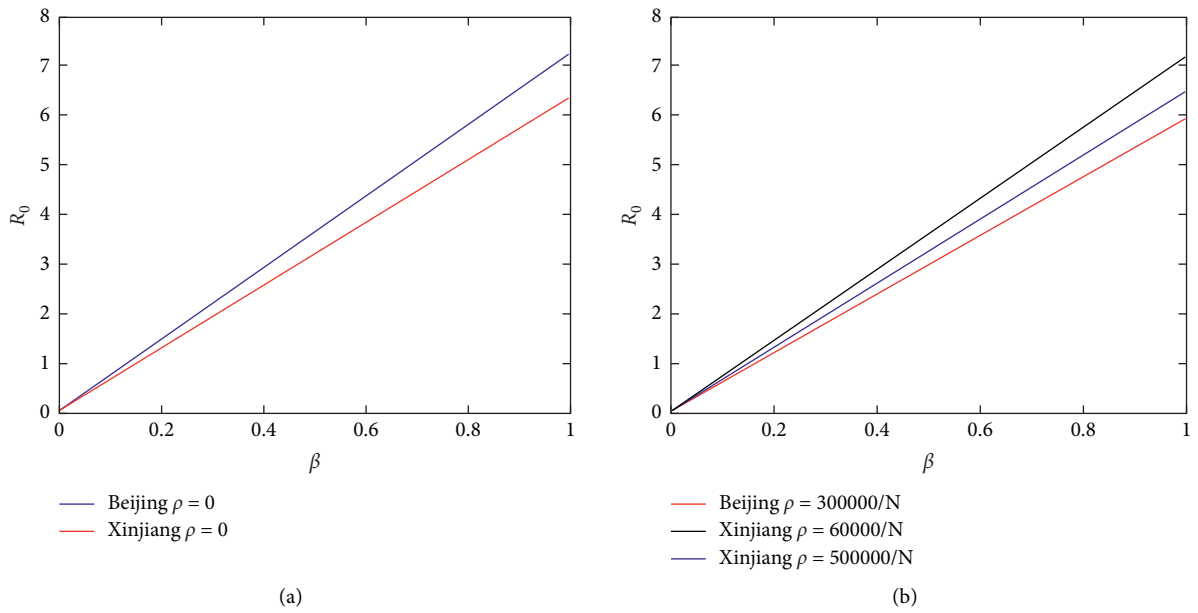

Figure 4: Continued.

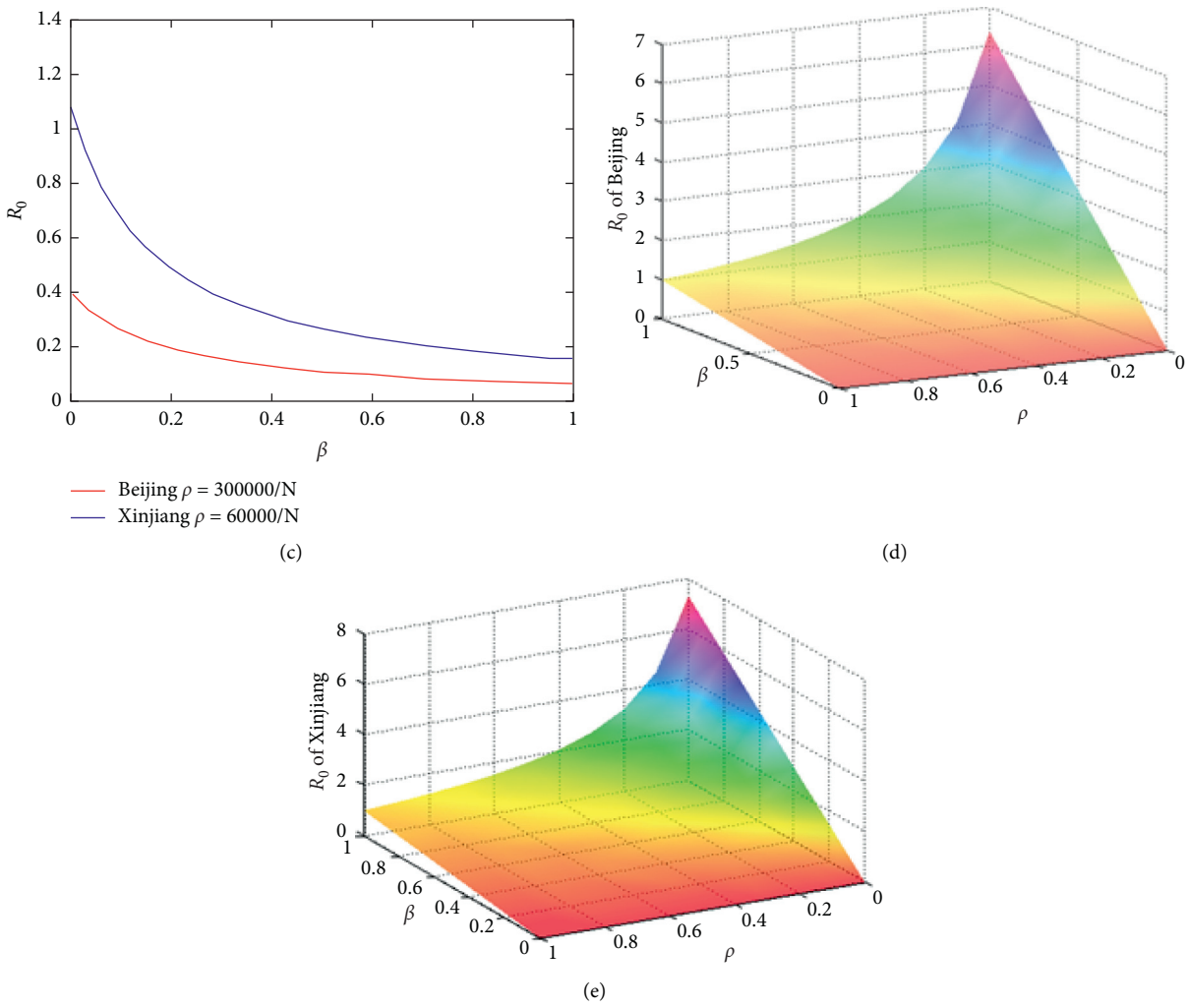

Figure 4: (a) R_0 in terms of β. (b) R_0 in terms of ρ. (c) R_0 in terms ofρ. (d) R_0 in terms of β and ρ for Beijing. (e) R_0 in terms of β and ρ for Xinjiang.

by the size of the basic reproduction number R_0, that is, the DFE was globally asymptotically stable if $R_0 < 1$, while an endemic equilibrium existed uniquely and was globally asymptotically stable if $R_0 > 1$. Based on mathematical analysis, data fitting, and sensitivity analysis, we revealed the effects of mass testing and quarantine. Without the mass vaccination campaign of COVID-19, it was found that the higher the mass testing is, the earlier the source of infection was determined for effectively controlling the spread. In addition, a larger coefficient of quarantine was necessary to control the spread of COVID-19. It was more effective in increasing the coefficient of quarantine if the population density of the region was less. If the government implements mass testing and quarantine, it must devote a large amount of continuous manpower, material, and financial resources to eliminate the epidemic. With the development of the vaccine for COVID-19, more people are vaccinated in a community, which makes it possible for eliminating the spread of COVID-19.

In the future, we plan to study the mass vaccination campaign for COVID-19 in the whole of China.

Data Availability

The data used to support the findings of this study are available from the corresponding author upon reasonable request (email: lifeng@sxau.edu.cn).

Conflicts of Interest

The authors declare that there are no conflicts of interest regarding the publication of this paper.

Acknowledgments

This work was supported by the National Natural Science Foundation of China (61873154), Shanxi Key Laboratory

(201705D111006), and Shanxi Scientific and Technology Innovation Team (201705D15111172) Grant.

References

[1] S. Ruan, "Likelihood of survival of coronavirus disease 2019," *The Lancet Infectious Diseases*, vol. 20, no. 6, pp. 630-631, 2020.

[2] "Centers for Disease Control and Prevention," http://www.nhc.gov.cn/.

[3] N. Zhu, D. Zhang, W. Wang et al., "A novel coronavirus from patients with pneumonia in China, 2019," *New England Journal of Medicine*, vol. 382, no. 8, pp. 727–733, 2020.

[4] C. Wang, P. W. Horby, F. G. Hayden, and G. F. Gao, "A novel coronavirus outbreak of global health concern," *The Lancet*, vol. 395, no. 10223, pp. 470–473, 2020.

[5] L. Pang, S. Liu, X. Zhang, T. Tian, and Z. Zhao, "Transmission dynamics and control strategies of COVID-19 in Wuhan, China," *Journal of Biological Systems*, vol. 415, pp. 1–18, 2020.

[6] B. Tang, X. Wang, Q. Li et al., "Estimation of the transmission risk of the 2019-nCoV and its implication for public health interventions," *Journal of Clinical Medicine*, vol. 9, no. 2, pp. 462–475, 2020.

[7] H. L. Smith, L. Wang, and M. Y. Li, "Global dynamics of an SEIR epidemic model with vertical transmission," *Siam Journal on Applied Mathematics*, vol. 62, pp. 58–69, 2001.

[8] H. W. Hethcote, "The mathematics of infectious diseases," *Siam Review*, vol. 42, no. 4, pp. 599–653, 2000.

[9] J. M. Heffernan, R. J. Smith, and L. M. Wahl, "Perspectives on the basic reproductive ratio," *Journal of the Royal Society Interface*, vol. 2, no. 4, pp. 281–293, 2005.

[10] A. Korobeinikov, "Global properties of basic virus dynamics models," *Bulletin of Mathematical Biology*, vol. 66, no. 4, pp. 879–883, 2004.

[11] P. Magal, O. Seydi, and G. Webb, "Final size of an epidemic for a two-group SIR model," *Siam Journal on Applied Mathematics*, vol. 76, no. 5, pp. 2042–2059, 2016.

[12] R. Subramanian, Q. He, and M. Pascual, "Quantifying asymptomatic infection and transmission of COVID-19 in New York City using observed cases, serology and testing capacity," *Proceedings of the National Academy of Sciences of the United States of America*, vol. 118, Article ID e2019716118, 2021.

[13] Q. Li, N. L. Bragazzi, S. Tang, Y. Xiao, B. Tang, and X. Wang, "Estimation of the transmission risk of the 2019-nCoV and its implication for public health interventions," *Journal of Clinical Medicine*, vol. 9, pp. 462–475, 2020.

[14] C. Yang and J. Wang, "Modeling the transmission of COVID-19 in the US - a case study," *Infectious Disease Modelling*, vol. 6, pp. 195–211, 2021.

[15] J. Arino and S. Portet, "A simple model for COVID-19," *Infectious Disease Modelling*, vol. 5, pp. 309–315, 2020.

[16] D. Fanelli and F. Piazza, "Analysis and forecast of COVID-19 spreading in China, Italy and France," *Chaos Solitons Fractals*, vol. 134, Article ID 109761, 2020.

[17] T. Chen, J. Rui, Q. Wang, Z. Zhao, J. Cui, and L. Yin, "A mathematical model for simulating the phase-based transmissibility of a novel coronavirus," *Infectious Diseases of Poverty*, vol. 9, pp. 24–32, 2020.

[18] Y. Chen, J. Cheng, Y. Jiang, and K. Liu, "A time delay dynamical model for outbreak of 2019-nCoV and the parameter identification," *Journal of Inverse and Ill-Posed Problems*, vol. 28, no. 2, pp. 243–250, 2020.

[19] G.-Q. Sun, S.-F. Wang, M.-T. Li et al., "Transmission dynamics of COVID-19 in Wuhan, China: effects of lockdown and medical resources," *Nonlinear Dynamics*, vol. 101, no. 3, pp. 1981–1993, 2020.

[20] L. Mangoni and M. Pistilli, *Epidemic Analysis of COVID-19 in Italy by Dynamical Modeling*, Social Science Electronic Publishing, Rochester, NY, USA, 2020.

[21] B. Tang, N. L. Bragazzi, Q. Li, S. Tang, Y. Xiao, and J. Wu, "An updated estimation of the risk of transmission of the novel coronavirus (2019-nCov)," *Infectious Disease Modelling*, vol. 5, pp. 248–255, 2020.

[22] M. O. Ibrahim, "A mathematical model for the epidemiology of tuberculosis with estimate of the basic reproduction number," *IOSR Journal of Mathematics*, vol. 5, pp. 46–52, 2013.

[23] P. van den Driessche and J. Watmough, "Reproduction numbers and sub-threshold endemic equilibria for compartmental models of disease transmission," *Mathematical Biosciences*, vol. 180, no. 1-2, pp. 29–48, 2002.

[24] N. P. Bhatia and G. P. Szeg¨o, *Dynamical Systems: Stability Theory and Applications*, Vol. 35, Springer, Berlin, Germany, 1967.

[25] J. P. LaSalle, "Stability of nonautonomous systems," *Nonlinear Analysis: Theory, Methods & Applications*, vol. 1, no. 1, pp. 83–90, 1976.

[26] M.-T. Li, G.-Q. Sun, Y.-F. Wu, J. Zhang, and Z. Jin, "Transmission dynamics of a multi-group brucellosis model with mixed cross infection in public farm," *Applied Mathematics and Computation*, vol. 237, pp. 582–594, 2014.

[27] J. P. LaSalle, *The Stability of Dynamical Systems*, Society for Industrial and Applied Mathematics, Philadelphia, PA, USA, 1976.

[28] L. Salle, Joseph, S. Lefschetz, and R. C. Alverson, *Stability by Liapunov's Direct Method with Applications*, Academic Press, Cambridge,, MA, USA, 1961.

[29] J. Ma, D. J. D. Earn, and J. D. David, "Generality of the final size formula for an epidemic of a newly invading infectious disease," *Bulletin of Mathematical Biology*, vol. 68, no. 3, pp. 679–702, 2006.

[30] L. Davidson, "An introduction to mathematical biology," *Development*, vol. 138, pp. 5269-5270, 2011.

[31] National Health Commission of the People's Republic of China, *Daily Report about 2019-nCov*, National Health Commission, Beijing, China, 2020, https://www.cdc.gov/coronavirus/2019-nCoV/index.html.

[32] H. Haario, M. Laine, A. Mira, and E. Saksman, "DRAM: efficient adaptive MCMC," *Statistics and Computing*, vol. 16, no. 4, pp. 339–354, 2006.

[33] D. Sinha, "Markov chain Monte Carlo: Stochastic simulation for Bayesian inference," *Journal of the American Statistical Association*, vol. 104pp. 422-423, 2nd edition, 2009.